The Plant Cell, Vol. 7, 2129–2138, December 1995

End-to-End Annealing of Plant Microtubules by the p86 Subunit of Eukaryotic Initiation Factor-(iso)4F

Jeffrey D. Hugdahl, Carol L. Bokros, and Louis C. Morejohn[1]

Department of Botany, University of Texas at Austin, Austin, Texas 78713

The p86 subunit of eukaryotic initiation factor-(iso)4F from wheat germ exhibits saturable and substoichiometric binding to maize microtubules, induces microtubule bundling in vitro, and is colocalized or closely associated with cortical microtubule bundles in maize root cells, indicating its function as a microtubule-associated protein (MAP). The effects of p86 on the growth of short, taxol-stabilized maize microtubules were investigated. Pure microtubules underwent a gradual length redistribution, an increase in mean length, and a decrease in number concentration consistent with an end-to-end annealing mechanism of microtubule growth. Saturating p86 enhanced the microtubule length distribution and produced significantly longer and fewer microtubules than the control, indicating a facilitation of annealing by p86. Confirmation of endwise annealing rather than of dynamic instability as the mechanism for microtubule growth was made using mammalian MAP2, which also promoted the redistribution of length, increase in mean length, and decrease in number concentration of taxol-stabilized maize microtubules. Enhancement of microtubule growth occurred concomitant with bundling by p86, indicating that an alignment of microtubules in bundles facilitated endwise annealing kinetics. The results demonstrate that nonfacile plant microtubules can spontaneously elongate by endwise annealing and that MAPs enhance the rate of annealing. The p86 subunit of eukaryotic initiation factor-(iso)4F may be an important regulator of microtubule dynamics in plant cells.

INTRODUCTION

During the plant cell cycle, microtubules are reversibly polymerized to form several functionally distinct arrays. These include the preprophase band that influences the plane of cytokinesis, the mitotic spindle that segregates chromosomes, the phragmoplast that forms the cytokinetic plate, and the interphase cortical array that regulates the orientation of cellulose microfibril deposition during cell wall formation. Thus, microtubules have critical roles in plant growth and development, because they regulate subcellular organization, cell division and polarity, and the developmental pattern of tissue and organ morphogenesis (Lloyd, 1991). Although it is clear from extensive microscopy studies that the plant microtubule cytoskeleton undergoes a temporal and spatial reorganization process, the types of microtubule kinetics operative in plant cells are poorly understood.

Microtubules are dynamic filamentous polymers composed mainly of the globular protein tubulin, a 100-kD heterodimer having similar α and β subunits, and lesser amounts of microtubule-associated proteins (MAPs) that alter microtubule polymerization and stability (Wiche et al., 1991; Fosket and Morejohn, 1992). Microtubules are formed by the head-to-tail polymerization of tubulin to form linear protofilaments, typically 13 of which are laterally associated in the polymer wall (Amos, 1979). Microtubules have intrinsic dynamic properties that depend on the hydrolysis of GTP (Davis et al., 1994) and the binding of MAPs during polymerization (Wiche et al., 1991), and these dynamics are critically important for the reversible formation and continuous function of microtubules in various arrays assembled during the cell cycle (Gelfand and Bershadsky, 1991; Morejohn, 1991).

Microtubules deficient in MAP content are dynamically unstable and exist as populations of microtubules slowly growing and rapidly shrinking at their plus ends (Mitchison and Kirschner, 1984; Horio and Hotani, 1986). Dynamically unstable microtubules in vitro gradually increase in length and decrease in number, with the total mass of polymer remaining unchanged (Gelfand and Bershadsky, 1991). Microtubules having a relatively high MAP content are not dynamically unstable and thus do not exhibit appreciable changes in length or number (Margolis and Wilson, 1978; Hotani and Horio, 1988; Drechsel et al., 1992; Yamauchi et al., 1993; Itoh and Hotani, 1994). However, MAP-saturated microtubules are kinetically active and engage in treadmilling, that is, the addition of dimers to plus ends is balanced by the subtraction of dimers from minus ends, resulting in the directional flux of dimers from the plus ends to the minus ends (Margolis and Wilson, 1978; Hotani and Horio, 1988). Both dynamic instability and treadmilling of microtubules have been observed in animal cells (Schulze and Kirschner, 1986; Cassimeris et al., 1988; Mitchison, 1989).

[1] To whom correspondence should be addressed.

Another kinetic process of microtubule growth that may predominate under certain conditions is the end-to-end joining or annealing of microtubules. Annealing may occur rapidly and with sufficient magnitude that it can give rise to large increases in microtubule growth and a reduction in microtubule number concentration within a short period (Caplow et al., 1986; Rothwell et al., 1986, 1987; Williams and Rone, 1988, 1989). Stabilization of microtubules by taxol slows the rate of annealing only slightly, indicating a minor dependence of annealing on the dynamic state of microtubule ends (Rothwell et al., 1986; Williams and Rone, 1989). As the initial polymer length is decreased and/or polymer number concentration is increased, the rate of microtubule annealing increases; annealing has been proposed to be most efficient when microtubules have an aligned orientation, as when bundled (Caplow et al., 1986; Rothwell et al., 1986; Williams and Rone, 1989). Although annealing of animal microtubules occurs in the presence or absence of MAPs (Caplow et al., 1986; Rothwell et al., 1986), the effects of MAPs or bundling on microtubule annealing have not been examined.

Selected components of the protein translational machinery have been shown to interact with microtubules in vitro and in cells, suggesting that the regulation of protein synthesis and cytoskeletal organization are functionally interrelated and coordinately regulated (Condeelis, 1995; St. Johnston, 1995). We have shown recently that the p86 subunit of eukaryotic initiation factor–(iso)4F [eIF-(iso)4F] from wheat germ has several characteristics of a MAP (Bokros et al., 1995). eIF-(iso)4F is a complex of equimolar amounts of a p28 subunit that binds the 7-methylguanine cap of mRNA and a p86 subunit that is essential for in vitro translation but whose specific function during translation initiation is unknown (Browning et al., 1992). The p86 subunit but not the p28 subunit of eIF-(iso)4F binds and bundles microtubules in vitro. In maize root cells, p86 is diffusely distributed not only as fine particles throughout the cytosol but also as coarse particles and linear patches either colocalized or closely associated with cortical microtubule bundles. Thus, the p86 subunit of eIF-(iso)4F is a novel MAP that may link the protein synthesis machinery and mRNAs to microtubules and/or regulate the disposition of microtubules in plant cells (Bokros et al., 1995).

Recently, Brandt and Lee (1994) used both microtubule bundling and nonbundling forms of the mammalian neuronal MAP *tau* to examine the effect of bundling on microtubule behavior in vitro. They found that microtubules in bundles elongated 30% faster than microtubules not organized in bundles. They also found that microtubule assembly and bundling occurred simultaneously, suggesting a close relationship between the two processes (Brandt and Lee, 1994). Because the efficiency of microtubule annealing may increase when microtubules are aligned (Caplow et al., 1986; Rothwell et al., 1986), the results of Brandt and Lee (1994) suggested to us that microtubules in bundles may grow faster than nonoriented microtubules as a result of endwise annealing. This idea, together with the knowledge that the p86 subunit of eIF-(iso)4F bundled microtubules (Bokros et al., 1995), motivated our present study to determine whether p86 affected the annealing of plant microtubules in vitro.

RESULTS

Effects of p86 on the Disposition of Microtubules

Microtubule annealing experiments were performed by breaking taxol-stabilized maize microtubules with mechanical shearing. This increases the number of microtubules (and their ends) available for endwise joining and decreases the length of microtubules, which affords more rotational freedom of polymer in solution (Caplow et al., 1986; Rothwell et al., 1987; Williams and Rone, 1988, 1989). We have shown previously that maize tubulin has a very low critical concentration (C_c) in the presence of a molar excess taxol, with virtually all dimers being polymerized into microtubules at steady state (Bokros et al., 1993). For experiments described here, maize tubulin was found to have a C_c of 0.4 μM at 25°C in an approximately threefold molar excess of taxol to tubulin, and polymer sedimentation analysis of microtubules following shearing revealed no discernible microtubule depolymerization (see Methods).

Sheared taxol-stabilized microtubules (4 μM tubulin) were mixed either with assembly buffer (control) or with wheat germ p86 (1 μM) and incubated continuously at 25°C. Following sedimentation of microtubules by centrifugation, SDS-PAGE analysis was performed on supernatant and pellet fractions. The results revealed that virtually no tubulin dimer existed in the supernatant fraction and that essentially all available tubulin was polymerized into microtubules in the pellet fraction (Figure 1). In addition, most of the p86 was bound to sedimented microtubules, with excess unbound p86 remaining in the supernatant (Figure 1). Trace amounts of minor polypeptides in the p86 preparation also bound to microtubules, and immunoblotting with an affinity-purified antibody against p86 (Bokros et al., 1995) showed them to be proteolytic products of p86 (data not shown). Quantitative gel densitometry showed that 1 mol p86 bound per 5.5 mol tubulin in microtubules, indicating that all available p86 binding sites on microtubules were occupied (Bokros et al., 1995).

Microtubule dynamics were quantified by recording microtubule lengths at different times (0, 5, 10, 30, and 60 min) using negative-stain electron microscopy. Examples of microtubules incubated for 30 min in the absence or presence of p86 are given in Figure 2. Control microtubules were haphazardly arranged throughout the experiment and appeared longer at each time point, indicating that an endwise joining of microtubules had occurred. In the presence of p86, microtubules were haphazardly arranged at the earliest time point (0 min), but at all later time points microtubules were oriented in parallel, forming either short loosely packed bundles or long densely packed cables. In addition, p86-saturated microtubules appeared longer than control microtubules at most time points (Figure 2).

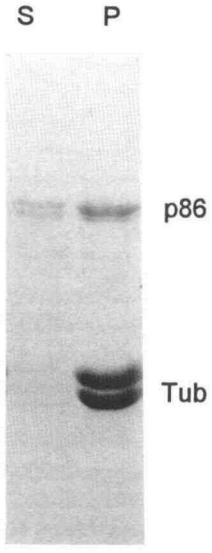

Figure 1. SDS-PAGE Analysis of the Binding of Wheat Germ p86 Subunit of eIF-(iso)4F to Taxol-Stabilized Microtubules.

Lanes of the Coomassie blue–stained gel contain the supernatant (S) and pellet (P) protein fractions resulting from the sedimentation of sheared taxol-stabilized microtubules incubated with p86. Positions of p86 and tubulin (Tub) are indicated.

p86 Enhancement of Microtubule Length Redistribution

To quantify the redistribution of microtubule length following shearing, measurements were made of microtubules at each time point, and the data are presented as histograms in Figure 3. The analysis showed that the control microtubule reaction initially consisted of a narrow length distribution of short microtubules that was gradually converted to a wide length distribution of longer microtubules, consistent with microtubule growth by endwise annealing. Interestingly, p86-saturated microtubules underwent a more rapid and extensive length redistribution than the control (Figure 3). The data indicated that the rate of microtubule annealing was promoted by p86.

p86 Enhancement of Mean Microtubule Length Increase

For control microtubules and p86-saturated microtubules, the mean microtubule length and number concentration were determined at each time point and the data are presented in Figure 4 and Table 1, respectively. No significant changes in mean microtubule length were found in either sample within 5 min, but gradual increases in microtubule length (Figure 4) and decreases in microtubule number concentration (Table 1) were found in both samples at 15, 30, and 60 min. The results showed that within 60 min, the mean length of control microtubules doubled from 0.85 ± 0.42 to 1.76 ± 0.92 μm (Figure 4), and the microtubule number concentration decreased more than twofold from 24.0 to 11.6 × 10^{-10} M (Table 1). During the same period, the mean length of p86-saturated microtubules tripled from 0.87 ± 0.44 to 2.63 ± 1.53 μm (Figure 4), and the microtubule number concentration decreased nearly threefold from 26.0 to 8.6 × 10^{-10} M (Table 1). The enhancement of microtubule growth by p86 was statistically significant ($P < 0.001$) at 15, 30, and 60 min. Thus, within 60 min, the extent of microtubule growth with p86 (~1.76 μm) was ~1.9-fold greater than that of the control (~0.91 μm).

Effects of MAP2 on the Disposition of Microtubules

An alternative explanation for the observed p86 enhancement of microtubule growth was that p86 binding to microtubules may have produced the unexpected and unusual effects of destabilizing taxol-stabilized microtubules and reactivating

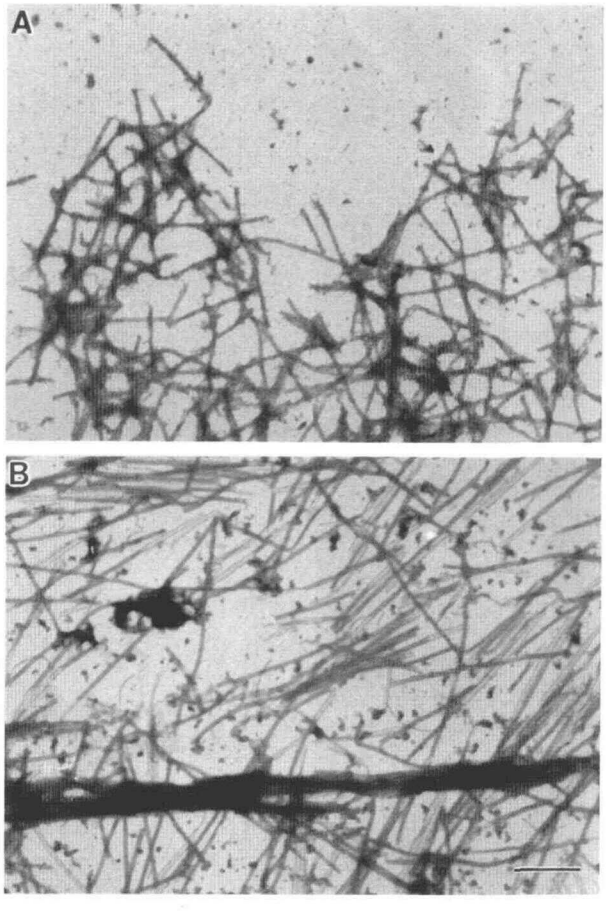

Figure 2. Effects of Saturating p86 on the Disposition of Taxol-Stabilized Microtubules.

(A) Microtubules incubated for 60 min with buffer alone.
(B) Microtubules incubated for 60 min with saturating p86.
Bar in **(B)** = 0.5 μm for **(A)** and **(B)**.

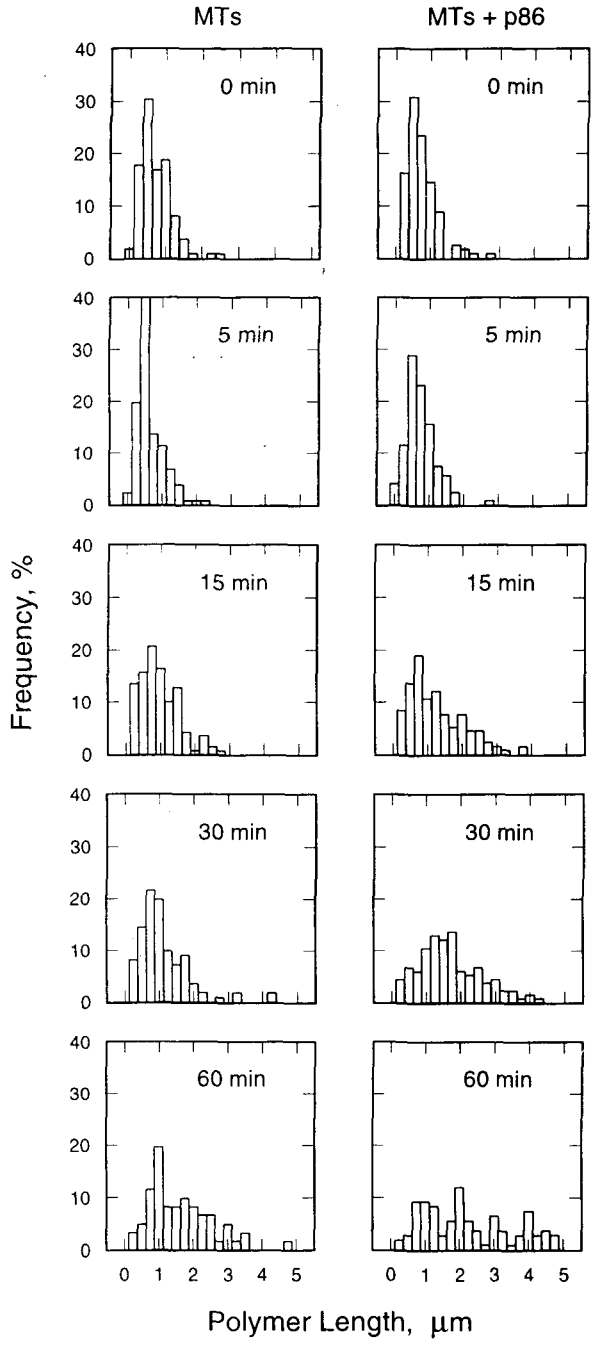

Figure 3. Microtubule Length Redistribution in the Absence or Presence of p86.

For sheared microtubules (MTs) incubated alone or with saturating p86 (MTs + p86), the frequency (%) of polymers observed in each 0.25-μm length category is presented for the indicated times.

dynamic instability. This would result in a greater microtubule length redistribution and mean microtubule length change than with control microtubules, consistent with the data in Figures 3 and 4. We tested this possibility by repeating the maize microtubule growth experiments in the absence and presence of MAP2, a well-characterized mammalian fibrous MAP that stabilizes microtubules and inhibits the microtubule length redistribution and length increase associated with dynamic instability kinetics (Hotani and Horio, 1988; Kowalski and Williams, 1993; Wallis et al., 1993; Yamauchi et al., 1993; Itoh and Hotani, 1994). MAP2 binds to the same number of saturable sites on preformed, taxol-stabilized microtubules from plants and bovine brain, albeit with different affinities (Hugdahl et al., 1993; Hugdahl and Morejohn, 1994).

Sheared taxol-stabilized maize microtubules (5 μM tubulin) were mixed either with assembly buffer (control) or with MAP2 (5 μM), and samples were incubated at 25°C. SDS-PAGE analysis and quantitative gel densitometry of supernatant and pellet fractions from sedimented microtubules revealed that all detectable tubulin was assembled and that MAP2 bound to microtubules, with 1 mol MAP2 per 6.6 mol tubulin (data not shown). These results were nearly identical with those we obtained previously with unsheared microtubules (Hugdahl et al., 1993). The negative-stain electron microscopy showed

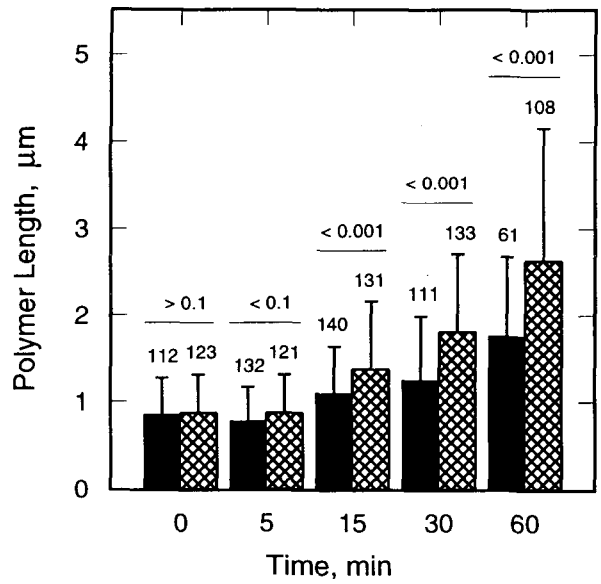

Figure 4. Changes in Mean Microtubule Length in the Absence or Presence of p86.

The mean length of microtubules incubated alone (solid bars) or with p86 (crosshatched bars) is presented for the indicated times. The standard deviation of the mean microtubule length for each sample is represented by a vertical line on each bar, and the total number of microtubules measured is indicated above each vertical line. The significance level (P) of the difference between the mean lengths of control and p86-saturated microtubules at each time point is shown above each pair of bars.

Table 1. Changes in Microtubule Number Concentration in the Absence or Presence of p86

Time (min)	Microtubule Number Concentration ($\times 10^{-10}$ M)	
	Control	p86
0	24.0	26.0
5	26.1	26.0
15	18.5	16.4
30	16.3	12.5
60	11.6	8.6

randomly arranged microtubules in both the control and MAP-containing samples, and no microtubule bundles were formed, as previously reported (Matus, 1994; Bokros et al., 1995). However, MAP2-saturated microtubules appeared longer than control microtubules at corresponding time points (data not shown), as was seen with p86-saturated microtubules (Figure 2).

MAP2 Enhancement of Microtubule Length Redistribution and Mean Length Increase

Maize microtubule length redistributions in the absence and presence of MAP2 were plotted from microtubule measurements obtained at each time point. Histogram analyses showed that a narrow length distribution of control microtubules was gradually replaced by a wider length distribution (Figure 5), a result similar to that observed in the previous control microtubule sample (Figure 3). MAP2-saturated microtubules underwent a more extensive length redistribution than control microtubules (Figure 5), consistent with microtubule growth by end-to-end annealing (Caplow et al., 1986; Rothwell et al., 1986) but not by dynamic instability (Hotani and Horio, 1988; Yamauchi et al., 1993; Itoh and Hotani, 1994).

Changes in microtubule mean length and number concentration were determined in the absence and presence of MAP2, and the results are presented in Figure 6 and Table 2, respectively. Within 60 min, the mean length of control microtubules increased 1.8-fold from 0.93 ± 0.38 to 1.70 ± 0.9 μm (Figure 6), and the microtubule number concentrations decreased from 28.0 to 15.3 × 10^{-10} M (Table 2). In the same period, the mean length of MAP2-saturated microtubules increased 2.1-fold from 1.07 ± 0.38 to 2.26 ± 1.38 μm (Figure 6), and the microtubule number concentration decreased from 26.5 to 12.5 × 10^{-10} M (Table 2). Differences between mean microtubule lengths of control microtubules and MAP2-saturated microtubules were significant ($P < 0.001$) at all time points. Thus, the extent of microtubule growth with MAP2 (~1.19 μm) was ~1.5-fold greater than the control (~0.77 μm), consistent with a MAP2-enhanced annealing of taxol-stabilized microtubules. The similar effects of p86 and MAP2 on the patterns of maize microtubule growth indicated that both p86 and MAP2 stabilize microtubules and enhance the growth of nonfacile microtubules by end-to-end annealing.

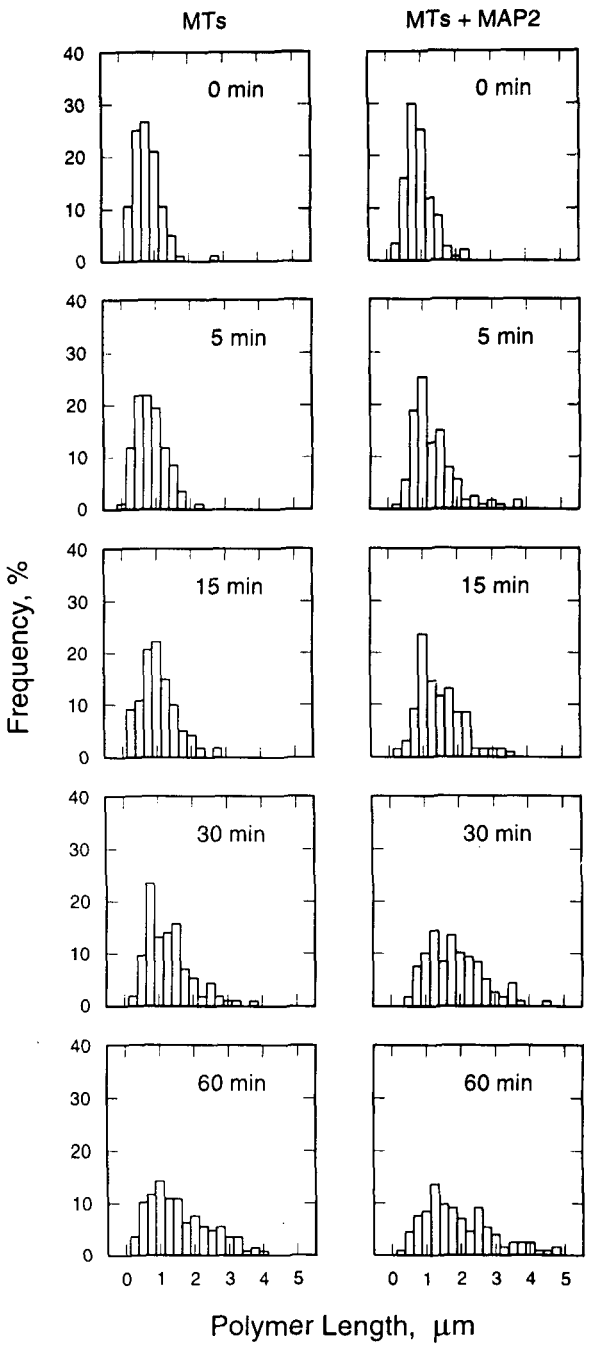

Figure 5. Microtubule Length Redistribution in the Absence or Presence of MAP2.

For sheared microtubules (MTs) incubated alone or with saturating MAP2 (MTs + MAP2), the frequency (%) of polymers observed in each 0.25-μm length category is presented for the indicated times.

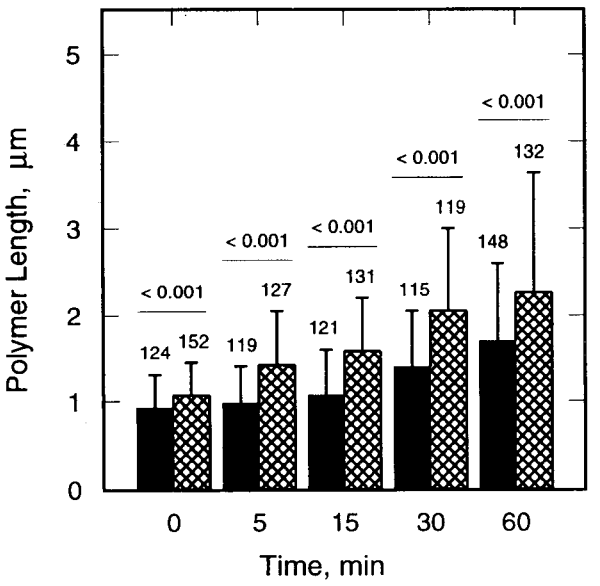

Figure 6. Changes in Mean Microtubule Length in the Absence or Presence of MAP2.

The mean length of microtubules incubated alone (solid bars) or with MAP2 (crosshatched bars) is presented for the indicated times. The standard deviation of the mean microtubule length for each sample is represented by a vertical line on each bar, and the total number of microtubules measured is indicated above each vertical line. The significance level (P) of the difference between the mean lengths of control and MAP2-saturated microtubules at each time point is shown above each pair of bars.

The slightly greater extent of microtubule annealing induced by p86 than by MAP2 suggested that p86-induced microtubule bundling enhanced annealing. At each time point, the extent of microtubule bundling in the absence (control) or presence of p86 and MAP2 was estimated qualitatively; the observations are summarized in Table 3. The data show that during annealing, no bundling of microtubules occurred in the absence or presence of MAP2 but that p86-saturated microtubules were moderately bundled within 5 min and remained extensively bundled thereafter (Table 3). The close correspondence between the temporal development of bundles (Table 3) and the p86-induced increases in mean microtubule length (Figure 4) and decreases in microtubule number concentration (Table 1) are consistent with an enhancement of annealing concomitant with bundle formation.

DISCUSSION

Conditions Affecting Microtubule Annealing Kinetics in Vitro

Microtubule kinetics of treadmilling and dynamic instability rely on relatively rapid dimer exchange rates between an unassembled tubulin pool and microtubule ends. Both treadmilling and dynamic instability of mammalian microtubules are dramatically inhibited by taxol (Kumar, 1981; Caplow and Zeeberg, 1982; Wilson et al., 1985; Deery et al., 1995). Thus, in the presence of taxol, animal microtubule elongation must occur by an endwise annealing mechanism (Williams and Rone, 1988, 1989). Although taxol's effects on maize microtubule treadmilling and dynamic instability have not been examined directly, taxol must also strongly suppress these dynamics, because the C_c of maize tubulin is reduced from 8.3 to 0.6 µM by a stoichiometric molar excess of taxol (Bokros et al., 1993). Thus, so little plant dimer remains unassembled in the presence of taxol that microtubule elongation could not occur by mechanisms requiring efficient endwise dimer exchange. Moreover, the binding of p86 or MAP2 to taxol-stabilized maize microtubules further reduces the maize tubulin C_c such that virtually no dimer remains unpolymerized (Figure 1; Hugdahl et al., 1993). Therefore, under our experimental conditions, the observed microtubule length increases must have resulted from an end-to-end annealing mechanism.

Our present data suggest that p86 promotes more efficient microtubule annealing than does MAP2, despite evidence that p86 has a lower affinity than MAP2 for binding to maize microtubules (Hugdahl et al., 1993; Bokros et al., 1995). This may stem from a combination of differences between the interactions of p86 and MAP2 with microtubules. First, p86 aligns microtubules in bundles in vitro, but MAP2 does not (Hugdahl and Morejohn, 1994; Matus, 1994; Bokros et al., 1995), and annealing appears to occur more readily with aligned microtubules than with nonaligned microtubules. Intuitively, this is because a freely rotating individual microtubule whose end collides with a bundle of microtubules is more likely to become coaligned with the bundled microtubules than if it contacts another free individual microtubule. Coaligned microtubules would have the most effective orientation for bonding of dimers exposed at each microtubule end. Also, p86 may better "seal" the junction formed at microtubule ends than MAP2, because the microtubule-binding domain of p86 may be larger than that of MAP2. The mass of the eIF-(iso)4F holoenzyme has been estimated to be ~330 kD (Bokros et al., 1995). Because p86 has the same binding stoichiometry to polymerized maize tubulin (1:5 to 6), whether examined in

Table 2. Changes in Microtubule Number Concentration in the Absence or Presence of MAP2

	Microtubule Number Concentration ($\times 10^{-10}$ M)	
Time (min)	Control	MAP2
0	28.0	26.5
5	26.6	19.9
15	24.3	17.9
30	18.6	13.8
60	15.3	12.5

Table 3. Time-Dependent Bundling of Microtubules during Annealing

Time (min)	Control	p86	MAP2
0	–	–	–
5	–	+ +	–
10	–	+ + +	–
30	–	+ + +	–
60	–	+ + +	–

Microtubule bundling was scored qualitatively as none (–), some (+), moderate (+ +), or extensive (+ + +).

the form of native eIF-(iso)4F or bacterially expressed p86 or p86–p28 complex (Bokros et al., 1995), p86 may exist as a trimeric molecule whose microtubule-binding domain covers 15 to 18 dimers on microtubules. The MAP2 molecule, however, is thought to be a monomer whose microtubule-binding domain binds to an estimated six to eight dimers on maize microtubules (Wiche et al., 1991; Hugdahl et al., 1993). Thus, p86 may more effectively decrease the dissociation rate of newly joined microtubules than MAP2, because its microtubule-binding domain may form a larger overlap of both microtubule ends at the annealing site.

Our experiments demonstrated that, as a result of annealing, the mean lengths of taxol-stabilized microtubules composed of pure maize tubulin approximately doubled within 60 min. This observation is remarkably similar to that obtained by Williams and Rone (1988, 1989), who reported an approximate doubling of the mean lengths of taxol-stabilized microtubules composed of pure bovine brain tubulin. Interestingly, Rothwell et al. (1986) reported that taxol reduced only slightly the extent of animal microtubule annealing, indicating that the kinetic properties of microtubule ends do not strongly influence the rate of microtubule annealing. Thus, the single most important factor contributing to microtubule growth by an annealing mechanism may be microtubule alignment. This idea is consistent not only with our current observation that microtubule annealing occurred concomitant with p86-induced bundling, but also with the results of Brandt and Lee (1994), who found that a bundling form of *tau* promoted microtubule elongation 30% faster than a nonbundling form of *tau*. It appears, therefore, that in the absence of taxol, microtubule elongation probably occurs via both endwise dimer addition and annealing mechanisms, as suggested previously (Caplow et al., 1986; Williams and Rone, 1988, 1989), but that bundling enhances significantly the contribution of annealing to microtubule growth.

The probability that microtubules will elongate by annealing increases with the number concentration of short microtubules (Rothwell et al., 1987; Williams and Rone, 1988, 1989). In fact, rapid increases in microtubule number concentration may be achieved by microtubule severing factors that have been shown to transform relatively few long microtubules into many short microtubules (Vale, 1991; Shiina et al., 1992, 1994). The fate of newly formed short microtubules may vary, depending on the conditions. For example, in the absence of taxol, short microtubules that are deficient in MAPs and unstable may completely depolymerize into tubulin dimer from their newly created plus ends (Hotani and Horio, 1988; Drechsel et al., 1992; Kowalski and Williams, 1993; Itoh and Hotani, 1994). Alternatively, short microtubules that are stabilized by MAPs may regrow both by endwise dimer addition and annealing, with the relative contribution of each mechanism depending on the concentrations of unassembled dimer and microtubules, respectively, and the extent of microtubule bundling.

Considerations of Microtubule Annealing in Vivo

Microtubule bundles are formed by the parallel orientation and close packing of microtubules, and they are functionally significant structures for the organizational integrity of the cytosolic compartment and the concerted directional transport of subcellular components. Both the formation of bundles and the spacing between microtubules in bundles are thought to be regulated by MAPs. Because we have colocalized p86 to cortical microtubule bundles in maize root cells (Bokros et al., 1995), p86 may be involved in regulating microtubule bundling and growth by annealing.

In cells having abundant numbers of aligned microtubules, endwise annealing of microtubules may be facilitated not only by MAPs but also by an unpolymerized dimer pool. This is because discontinuities that exist in the polymer lattice at annealing sites may be rapidly repaired by intercalation of unassembled dimer. Thus, microtubule annealing in vivo may be considerably more efficient than our in vitro experiments suggest is possible. Moreover, in plant cells, the relative contribution of annealing to overall microtubule growth may be substantial when microtubules are coaligned in dense bundles, such as those commonly observed in the cortical interphase array (Lloyd, 1991; Baluska et al., 1992; Yuan et al., 1994).

Recent studies of microtubule dynamics in plant cells microinjected with fluorescently labeled tubulin have shown that microtubules undergo rapid length changes (Wasteneys et al., 1993; Yuan et al., 1994). These changes occur not only to individual microtubules (Wasteneys et al., 1993) but also to microtubules arranged in bundles (Yuan et al., 1994). Microtubules in plant cells are also capable of bidirectional elongation during recovery from depolymerization and may undergo small translocations (Wasteneys et al., 1993). These observations further suggest that plant microtubule elongation could occur simultaneously by endwise dimer addition and microtubule annealing. Thus, microtubule growth by annealing may be most significant during the gradual reorientations that occur in parallel arrays of cortical microtubule bundles during cell elongation and differentiation (Baluska et al., 1992; Yuan et al., 1994). Further high-resolution observations of microtubule dynamics in vivo are necessary to assess the contribution of microtubule annealing to the dynamic reorganization of plant microtubule arrays.

METHODS

Purification of Maize Microtubules and Wheat Germ p86

Maize tubulin was isolated from stationary phase–cultured cells (*Zea mays* cv Black Mexican Sweet) by DEAE chromatography, as described previously (Morejohn and Fosket, 1982; Bokros et al., 1993). Tubulin (10 μM) polymerization was performed in a buffer composed of 50 mM Pipes-KOH, pH 6.9, 1 mM EGTA, 0.5 mM $MgSO_4$, 1 mM DTT, 1 mM GTP, 20 μM taxol, 2% (v/v) dimethyl sulfoxide, and the following protease inhibitors: 50 μg/mL *Nα-p*-tosyl-L-arginine methyl ester and 1 μg/mL each of leupeptin hemisulfate, pepstatin A, and aprotinin (Sigma). Tubulin was polymerized into microtubules using a gradual temperature ramping protocol, and microtubules were purified to homogeneity by centrifugation at 30,000*g* (TLA-100 rotor and TL-100 ultracentrifuge; Beckman Instruments) for 40 min (25°C) through a 20% (w/v) sucrose cushion containing 1 μM taxol and 1% (v/v) DMSO (Bokros et al., 1993; Hugdahl et al., 1993).

The bacterially expressed p86 subunit of wheat germ eukaryotic initiation factor–(iso)4F [eIF-(iso)4F] was isolated by phosphocellulose chromatography, as described by van Heerden and Browning (1994) and equilibrated in assembly buffer, as described by Bokros et al. (1995). The p86 preparation contains a very low level of impurities that had no effect on p86 binding to microtubules.

Isolation of Bovine Brain Microtubule-Associated Protein 2

Microtubule-associated protein 2 (MAP2) was isolated as a heat-stable protein from the supernatant of bovine brain extract (Hugdahl et al., 1993), with modifications as described by Hugdahl and Morejohn (1994). Quantitative densitometry of Coomassie blue–stained gels afforded >40% MAP2, of which >95% was competent to bind microtubules. Although *tau* and other polypeptides were present in the MAP preparation, microtubule sedimentation and SDS-PAGE of the supernatant and pellet fractions showed that only MAP2 bound to maize microtubules. Immediately before use, a MAP2 sample was thawed and clarified of insoluble materials at 160,000*g* (20°C) for 30 min in a Beckman TL-100 ultracentrifuge (TLA-100 rotor).

Protein Determinations, Gel Electrophoresis, Quantitative Gel Densitometry, and Microtubule Sedimentation

Protein assays (Bradford, 1976), SDS-PAGE (Laemmli, 1970), and quantitative densitometry of Coomassie blue–stained gels were performed as described by Hugdahl et al. (1993). The molecular masses of wheat germ EF-1α p86 subunit of eIF-(iso)4F and maize tubulin were assumed to be 86 and 100 kD, respectively, on the basis of cDNA sequencing studies (Allen et al., 1992; Fosket and Morejohn, 1992). Microtubules were sedimented for 30 min (25°C) at 30,000*g* in a Beckman TLA-100 rotor and TL-100 ultracentrifuge.

Microtubule Annealing Reactions

The effects of p86 and MAP2 on the annealing of sheared taxol-stabilized microtubules were examined using a microtubule assembly buffer composed of 50 mM Pipes-KOH, pH 6.9, 1 mM EGTA, 0.5 mM $MgSO_4$, 1 mM DTT, 0.1 mM GTP, 10 μM taxol, 1% (v/v) dimethyl sulfoxide, and the following protease inhibitors: 50 μg/mL *Nα-p*-tosyl-L-arginine methyl ester and 1 μg/mL each of leupeptin hemisulfate, pepstatin A, and aprotinin. Taxol-stabilized microtubules (25 μM tubulin) were sheared by rapid trituration (10 to 20 times) through a 200-μL micropipette tip. Pilot electron microscopy observations showed this shearing method to produce short microtubules, typically having a length of 0.8 ± 0.4 μM. When pure taxol-stabilized microtubules were sheared and sedimented (30,000*g* for 30 min at 25°C), protein determinations on supernatant and pellet fractions revealed no detectable microtubule depolymerization. To initiate an annealing reaction, sheared taxol-stabilized microtubules were mixed in assembly buffer alone and with either p86 or MAP2 to provide final concentrations of 4 to 5 μM tubulin and either 1 μM p86 or 5 μM MAP2. Because ~1 mol taxol binds per mol tubulin in polymer (Parness and Horwitz, 1981; Derry et al., 1995), the sedimentation and resuspension of microtubules previously assembled with saturating taxol results in an increase in the final taxol concentration. Thus, annealing reactions were estimated to contain final taxol concentrations of ~14 to 15 μM after resuspension of taxol-stabilized maize microtubules to 4 to 5 μM tubulin. Microtubules were incubated in microfuge tubes at 25°C, and at appropriate times, 5 μL aliquots were gently withdrawn with a 200-μL micropipette tip, taking care not to disturb polymer with shearing forces, and processed for negative-stain electron microscopy.

Electron Microscopy and Microtubule Length Measurements

To examine microtubules by negative-stain electron microscopy, samples (5 μL) were placed on 200-mesh copper grids coated with Formvar and carbon (Ted Pella, Redding, CA) and allowed to adsorb to the grid surface for 1 min. The solution was removed by wicking with a filter paper, grids were rinsed for 15 sec with 5 μL of water, and adsorbed polymer was negatively stained for 1 min with 5 μL of 2% (w/v) uranyl acetate (Polysciences, Inc., Warrington, PA). Grids were briefly washed with 5 μL of water, wicked, and allowed to air dry. Microtubules were observed and photographed on a Jeol JEM-100CX electron microscope at 80 kV, and photographs were taken at a magnification of ×5500. Microtubule length was measured directly from electron microscopy negatives on a light box using a dissecting microscope, as described by Hugdahl et al. (1993). In annealing experiments with MAP2, microtubules were measured from enlarged prints. Care was taken to measure only those microtubules having both ends exposed, and microtubules in densely packed p86-induced bundles were not measured. All histogram analyses of microtubule redistribution were performed using microtubule length categories of 0.25 μm. The Student's *t* test was used to determine the statistical significance of differences between mean microtubule lengths.

To determine the microtubule number concentration at each time point, the concentration of polymerized maize tubulin was divided by the product of the number of dimers per micrometer and mean microtubule length (also in micrometers). Taxol-stabilized maize microtubules were assumed to contain an average of 14 protofilaments (Bokros et al., 1993) and thus 1766 dimers per micrometer (Amos, 1979). Quantitative densitometry of supernatant and pellet protein fractions analyzed by SDS-PAGE provided a C_c of 0.4 μM for pure maize tubulin in the presence of a molar excess of taxol, and virtually all detectable tubulin was polymerized in the presence of taxol and p86 or MAP2.

ACKNOWLEDGMENTS

We thank Virginia R. Hanesworth for excellent technical support, Dr. Karen S. Browning for generously providing the p86 subunit of eIF-

(iso)4F, and Dr. Doug Murphy and Dr. Robley Williams for their encouragement and helpful discussions. This research was supported by grants to L.C.M. from the National Science Foundation (No. MCB-8996274 and No. MCB-9415479) and the Institute for Cellular and Molecular Biology (University of Texas at Austin). C.L.B. was supported in part by Bess Heflin and R.A. Hutchison Fellowships, and J.D.H. was supported by a Plant Biology Postdoctoral Fellowship from the National Science Foundation (No. DIR-9104365). Electron microscopy was performed at the University of Texas Cell Research Institute.

Received June 9, 1995; accepted October 4, 1995.

REFERENCES

Allen, M.L., Metz, A.M., Timmer, R.T., Rhoads, R.E., and Browning, K.S. (1992). Isolation and sequence of the cDNAs encoding the subunits of the isozyme form of protein synthesis initiation factor 4F. J. Biol. Chem. **267,** 23232–23236.

Amos, L.A. (1979). Structure of microtubules. In Microtubules, K. Roberts and J.S. Hyams, eds (London: Academic Press), pp. 1–64.

Baluska, F., Parker, J.S., and Barlow, P.W. (1992). Specific patterns of cortical and endoplasmic microtubules associated with cell growth and tissue differentiation in roots of maize (*Zea mays* L.). J. Cell Sci. **103,** 191–200.

Bokros, C.L., Hugdahl, J.D., Hanesworth, V.R., Murthy, J.V., and Morejohn, L.C. (1993). Characterization of the reversible taxol-induced polymerization of plant tubulin into microtubules. Biochemistry **32,** 3437–3447.

Bokros, C.L., Hugdahl, J.D., Hanesworth, V.R., Kim, H.-H., van Heerden, A., Browning, K.S., and Morejohn, L.C. (1995). Function of the p86 subunit of eukaryotic initiation factor–(iso)4F as a microtubule-associated protein in plant cells. Proc. Natl. Acad. Sci. USA **92,** 7120–7124.

Bradford, M.M. (1976). A rapid and sensitive method for the quantitation of microgram quantities of protein utilizing the principle of protein dye binding. Anal. Biochem. **72,** 248–254.

Brandt, R., and Lee, G. (1994). Orientation, assembly, and stability of microtubule bundles induced by a fragment of tau protein. Cell Motil. Cytoskeleton **28,** 143–154.

Browning, K.S., Webster, C., Roberts, J.K.M., and Ravel, J.M. (1992). Identification of an isozyme form of protein synthesis initiation factor 4F in plants. J. Biol. Chem. **267,** 10096–10100.

Caplow, M., and Zeeberg, B. (1982). Dynamic properties of microtubules at steady state in the presence of taxol. Eur. J. Biochem. **127,** 319–324.

Caplow, M., Shanks, J., and Brylawski, B.P. (1986). Differentiation between dynamic instability and end-to-end annealing models for length changes of steady-state microtubules. J. Biol. Chem. **261,** 16233–16240.

Cassimeris, L., Pryer, N.K., and Salmon, E.D. (1988). Real-time observations of microtubule dynamic instability in living cells. J. Cell Biol. **107,** 2223–2331.

Condeelis, J. (1995). Elongation factor 1α, translation and the cytoskeleton. Trends Biochem. Sci. **20,** 169–170.

Davis, D., Sage, C.R., Dougherty, C.A., and Farrell, K.W. (1994). Microtubule dynamics modulated by guanosine triphosphate hydrolysis activity of β-tubulin. Nature **264,** 839–842.

Derry, W.B., Wilson, L., and Jordon, M.A. (1995). Substoichiometric binding of taxol suppresses microtubule dynamics. Biochemistry **34,** 2203–2211.

Drechsel, D.N., Hyman, A.A., Cobb, M.H., and Kirschner, M.W. (1992). Modulation of the dynamic instability of tubulin assembly by the microtubule-associated protein tau. Mol. Biol. Cell **3,** 1141–1154.

Fosket, D.E., and Morejohn, L.C. (1992). Structural and functional organization of tubulin. Annu. Rev. Plant Physiol. Plant Mol. Biol. **43,** 201–240.

Gelfand, V.I., and Bershadsky, A.D. (1991). Microtubule dynamics: Mechanism, regulation, and function. Annu. Rev. Cell Biol. **7,** 93–116.

Hasezawa, S., and Nagata, T. (1991). Dynamic organization of plant microtubles at the three distinct transition points during the cell cycle progression of synchronized tobacco BY-2 cells. Bot. Acta **104,** 206–211.

Horio, T., and Hotani, H. (1986). Visualization of the dynamic instability of individual microtubules by dark-field microscopy. Nature **321,** 605–607.

Hotani, H., and Horio, T. (1988). Dynamics of microtubules visualized by darkfield microscopy: Treadmilling and dynamic instability. Cell Motil. Cytoskeleton **10,** 229–236.

Hugdahl, J.D., and Morejohn, L.C. (1994). Deficient nucleation during co-polymerization of mammalian MAP2 and tobacco tubulin. Biochem. Mol. Biol. Int. **34,** 375–384.

Hugdahl, J.D., Bokros, C.L., Hanesworth, V.R., Aalund, G.R., and Morejohn, L.C. (1993). Unique functional characteristics of the polymerization and MAP binding regulatory domains of plant tubulin. Plant Cell **5,** 1063–1080.

Itoh, T.J., and Hotani, H. (1994). Microtubule-stabilizing activity of microtubule-associated proteins (MAPs) is due to increase in frequency of rescue in dynamic instability: Shortening length decreases with binding of MAPs onto microtubules. Cell Struct. Funct. **19,** 279–290.

Kowalski, R.J., and Williams, R.C. (1993). Microtubule-associated protein 2 alters the dynamic properties of microtubule assembly and disassembly. J. Biol. Chem. **268,** 9847–9855.

Kumar, N. (1981). Taxol-induced polymerization of purified tubulin. J. Biol. Chem. **256,** 10435–10441.

Laemmli, U.K. (1970). Cleavage of structural proteins during the assembly of the head of bacteriophage T4. Nature **227,** 680–685.

Lloyd, C. (1991). The Cytoskeletal Basis of Plant Growth and Form. (London: Academic Press).

Margolis, R.L., and Wilson, L. (1978). Opposite end assembly and disassembly of microtubules at steady state in vitro. Cell **13,** 1–8.

Matus, A. (1994). MAP2. In Microtubules, J.S. Hyams and C.W. Lloyd, eds (New York: Wiley-Liss, Inc.), pp. 155–166.

Mitchison, T. (1989). Polewards microtubule flux in the mitotic spindle: Evidence from photoactivation of fluorescence. J. Cell Biol. **109,** 637–652.

Mitchison, T., and Kirschner, M. (1984). Dynamic instability of microtubule growth. Nature **312,** 237–242.

Morejohn, L.C. (1991). The molecular pharmacology of plant tubulin and microtubules. In The Cytoskeletal Basis of Plant Growth and Form, C. Lloyd, ed (London: Academic Press), pp. 29–43.

Morejohn, L.C., and Fosket, D.E. (1982). Higher plant tubulin identified by self-assembly into microtubules in vitro. Nature **297,** 426–428.

Parness, J., and Horwitz, S.B. (1981). Taxol binds to polymerized tubulin in vitro. J. Cell Biol. **91,** 479–487.

Rothwell, S.W., Grasser, W.A., and Murphy, D.B. (1986). End-to-end annealing of microtubules in vitro. J. Cell Biol. **102,** 619–627.

Rothwell, S.W., Grasser, W.A., Baker, H.N., and Murphy, D.B. (1987). The relative contribution of polymer annealing and subunit exchange to microtubule dynamics in vitro. J. Cell Biol. **105,** 863–874.

Schulze, E., and Kirschner, M. (1986). Microtubule dynamics in interphase cells. J. Cell Biol. **102,** 1020–1031.

Shiina, N., Gotoh, Y., and Nishida, E. (1992). A novel homo-oligomeric protein responsible for an MPF-dependent microtubule-severing activity. EMBO J. **11,** 4723–4731.

Shiina, N., Gotoh, Y., Kubomura, N., Iwamatsu, A., and Nishida, E. (1994). Microtubule severing by elongation factor 1α. Science **266,** 282–285.

St. Johnston, D. (1995). The intracellular localization of messenger RNAs. Cell **81,** 161–170.

Vale, R.D. (1991). Severing of stable microtubules by a mitotically activated protein in *Xenopus* egg extracts. Cell **64,** 827–839.

van Heerden, A., and Browning, K.S. (1994). Expression in *Escherichia coli* of the two subunits of the isozyme form of wheat germ protein synthesis factor 4F. J. Biol. Chem. **269,** 17454–17457.

Wallis, K.T., Azhar, S., Rho, M.B., Lewis, S.A., Cowan, N.J., and Murphy, D.B. (1993). The mechanism of equilibrium binding of microtubule-associated protein 2 to microtubules. J. Biol. Chem. **268,** 15158–15167.

Wasteneys, G.O., Gunning, B.E.S., and Hepler, P.K. (1993). Microinjection of fluorescent brain tubulin reveals dynamic properties of cortical microtubules in living plant cells. Cell Motil. Cytoskeleton **24,** 205–213.

Wiche, G., Oberkanins, C., and Himmler, A. (1991). Molecular structure and function of microtubule-associated proteins. Int. Rev. Cytol. **124,** 217–273.

Williams, R.C., and Rone, L.A. (1988). End-to-end joining of microtubules: Kinetics in crowded solutions. Protoplasma **145,** 200–203.

Williams, R.C., and Rone, L.A. (1989). End-to-end joining of taxol-stabilized GDP-containing microtubules. J. Biol. Chem. **264,** 1663–1670.

Wilson, L., Miller, H.P., Farrell, K.W., Snyder, K.B., Thompson, W.C., and Purich, D.L. (1985). Taxol stabilization of microtubules in vitro: Dynamics of tubulin addition and loss at opposite microtubule ends. Biochemistry **24,** 5254–5262.

Yamauchi, P.S., Flynn, G.C., Marsh, R.L., and Purich, D.L. (1993). Reduction in microtubule dynamics in vitro by brain microtubule-associated proteins and by a microtubule-associated protein-2 second repeated sequence analogue. J. Neurochem. **60,** 817–826.

Yuan, M., Shaw, P.J., Warn, R.M., and Lloyd, C.W. (1994). Dynamic reorientation of cortical microtubules, from transverse to longitudinal, in living plant cells. Proc. Natl. Acad. Sci. USA **91,** 6050–6053.